Influence of spherical aberration on axial imaging of confocal reflection microscopy

Sheppard, Colin J.R.; Gu, Min; Brain, Keith; Zhou, Hao

DOI:
10.1364/AO.33.000616

Document Version
Publisher's PDF, also known as Version of record

Citation for published version (Harvard):
Sheppard, CJR, Gu, M, Brain, K & Zhou, H 1994, 'Influence of spherical aberration on axial imaging of confocal reflection microscopy', *Applied Optics*, vol. 33, no. 4, pp. 616-624. https://doi.org/10.1364/AO.33.000616

Influence of spherical aberration on axial imaging of confocal reflection microscopy

Colin J. R. Sheppard, Min Gu, Keith Brain, and Hao Zhou

The influence of spherical aberration on axial imaging of confocal reflection microscopy is investigated. In particular, the effects of lens aperture size and of the first three orders of spherical aberration are inspected. It is shown both theoretically and experimentally that the aberrated axial response can be improved by slightly reducing the lens aperture size. The experimental results concerning the effect of the tube length on the axial response and the aberration compensation are also given.

1. Introduction

Confocal scanning microscopy is a new technology.[1,2] It has many advantages over conventional microscopy. For example, confocal microscopy permits three-dimensional imaging for a thick object because it has a strong optical-sectioning property.[1] One usually investigates this property by considering the axial response (or the axial image) from a perfect reflector scanned along the axial direction[1,2]: the narrower the axial response, the higher the axial resolution in three-dimensional imaging.

In practice, however, the axial response is usually degraded because of spherical aberration caused when the refractive index of the specimen does not match that of the immersion medium.[3–7] If the mismatch of the refractive indices is small, a simple theoretical model can be used to describe the effect of the spherical aberration,[4] while a rigorous model has been developed elsewhere[5] for the case in which the mismatch is large. Spherical aberration can also occur when the objective is operated at an incorrect tube length. In our previous investigations,[4–6] the effects of these two sources of the aberration on the axial response have been calculated numerically. It has been shown[4] that in the presence of the spherical aberration the axial response exhibits considerable sidelobes, the amplitude of which is increased as aberration increases, and that the defocus, the primary, and the fifth-order spherical aberrations caused by the refractive-index mismatch can be compensated for by alteration of the effective tube length at which the objective is operated. Thus an optimized axial response with reduced sidelobes can be achieved. In addition, we have seen that the spherical aberration increases with radius over the aperture of the imaging lens,[4,5] so that the effect of the aberration can become less strong if the aperture of the lenses is slightly reduced.

This paper is the extension of our previous investigation.[4] After a brief description of our previous results, the effect of the lens aperture size on the axial response is first investigated in Section 2. Then we inspect, in Section 3, the axial response in the presence of the defocus, the primary, and the fifth-order spherical aberration. In Section 4 the experimental results concerning the axial response in the presence of the spherical aberration caused by the alteration of the tube length are described. We also qualitatively demonstrate the improvement in the aberrated axial response by the slight reduction of the lens aperture size.

2. Effect of the Lens Aperture Size

According to our previous discussion,[4,5] the axial response from a perfect reflector in a confocal system satisfying the sine condition can be expressed as

$$I(z) = \left| \int_0^{\alpha} R(\theta) P^2(\theta) \exp(i2kz \cos\theta) \sin\theta \cos\theta \, d\theta \right|^2, \quad (1)$$

where θ is the angle of convergence of a ray, α and $P(\theta)$ are the semiangular aperture and the pupil function of the lens, respectively, and $R(\theta)$ is the reflection coefficient of the object, which is equal to unity when the object is a perfect reflector. Here $k = 2\pi/\lambda$, where λ is the wavelength of the illumination light.

The authors are with the Department of Physical Optics, University of Sydney, New South Wales 2006, Australia.

Received 11 May 1993; revision received 3 August 1993.
0003-6935/94/040616-09$06.00/0.

For an aberration-free system, the pupil function $P(\theta)$ is constant, in which case the axial response can be derived analytically.[8] In practice, spherical aberration can be produced when the refractive index of the immersion material does not match that of the specimen.[4] The spherical aberration function can be derived, if the refractive-index mismatch is small, as

$$\Phi_A = A \sec \theta, \tag{2}$$

where A is a dimensionless parameter defined[4] as

$$A = kt\Delta n. \tag{3}$$

Here t is the thickness of the immersion layer, and Δn is the difference of the refractive indices between the immersion material and the specimen. In this case, the effect of the spherical aberration can be described by a complex pupil function given by

$$P(\theta) = \exp(i\Phi_A). \tag{4}$$

It has been shown that the axial response in the presence of the spherical aberration Φ_A becomes asymmetric with pronounced sidelobes. The intensity of the central peak is reduced, while its half-width is accordingly broadened.

Another spherical aberration source in a confocal system is caused by the alteration of the effective tube length at which the objective lens is operated, which, if the Helmholtz condition is satisfied, can be expressed as

$$\Phi_B = B \tan^2 \theta, \tag{5}$$

where B is a normalized parameter that includes optical parameters of the lens.[4] The complex pupil function is now given by

$$P(\theta) = \exp[i(\Phi_A + \Phi_B)]. \tag{6}$$

The aberration Φ_B can produce an effect on the axial response similar to that of the aberration Φ_A.[4] In addition, if the signs of the two aberration functions are chosen to be opposite, the effect of the aberrations can be reduced, which is called aberration compensation or aberration balance. The condition for compensation at small angles occurs at[4]

$$A = -3.75B. \tag{7}$$

The relationships of Φ_A and Φ_B to the convergence angle θ of a ray are shown in Fig. 1 for $A = 100$ and $B = 26.66$. We also include the difference of the two aberration functions under the condition of Eq. (7). It is seen that the aberration functions Φ_A and Φ_B increase appreciably when the angle is larger than approximately 35°, but that the aberration difference $\Phi_A + \Phi_B$ under the balanced condition ($A = 100$ and $B = -26.66$) is almost constant when the angle is less than approximately 50°. This conclusion suggests that it is possible to reduce the effect of the aberration by a slight reduction of the lens aperture size for a given value of A.

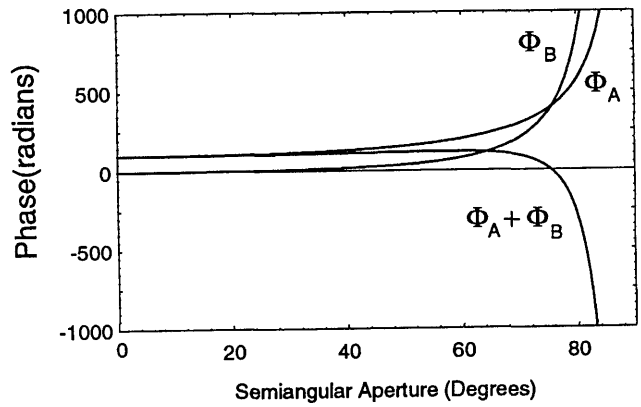

Fig. 1. Spherical aberrations as a function of angle θ when $A = 100$ for Φ_A, $B = 26.66$ for Φ_B, and $A = 100$ and $B = -26.66$ for $\Phi_A + \Phi_B$.

The axial response for the particular case in which $A = 100$ and $B = 0$ is investigated for different values of the semiangular aperture size α. This value of A corresponds to approximately $\Delta n = 0.04$ for an oil-immersion cover glass 0.17 mm thick when $\lambda = 0.6328$ μm. The half-width of the central peak and its intensity as a function of α are displayed in Figs. 2 and 3, respectively. It is evident that there is a decrease in the half-width of the central peak as α is increased until a minimum half-width is attained (see the curve for the unbalanced case in Fig. 2). Beyond this point the half-width is increased and oscillates to a constant value. This phenomenon is understandable from Fig. 1. When the aperture size is increased, there are two effects on the axial response: one is the decrease of the half-width because the numerical aperture of the lens is increased, and the other is the increase of the half-width because the aberration becomes strong. These two effects give a trade-off point for the axial response, meaning that one can optimize the axial response by altering the aperture size of the lens. The optimum value for the half-width occurs at an angle of ~35°, which corresponds to the value from which the change of the aberration Φ_A becomes pronounced (Fig. 1). This decreased half-width accordingly induces a maximum

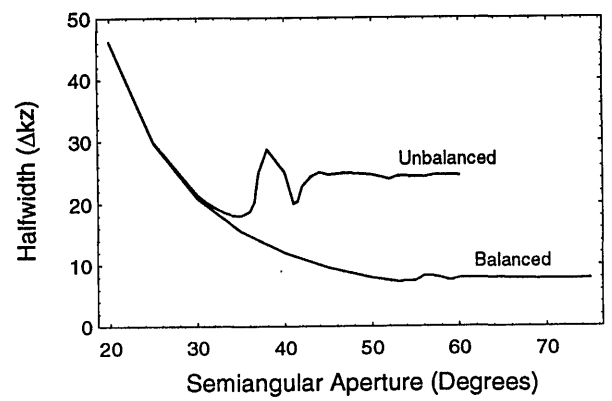

Fig. 2. Half-width as a function of the semiangular aperture α for unbalanced and balanced cases.

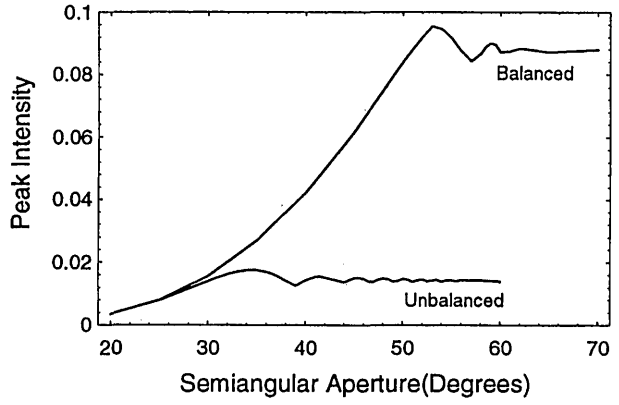

Fig. 3. Peak intensity as a function of the semiangular aperture α for unbalanced and balanced cases.

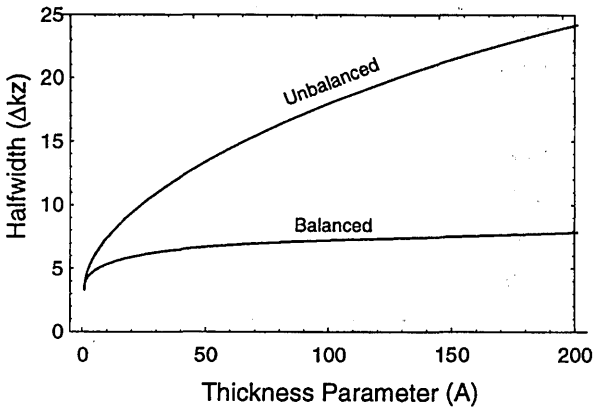

Fig. 5. Optimum half-width as a function of A for unbalanced and balanced cases.

in peak intensity as the aperture size increases (see the curve for the unbalanced case in Fig. 3). It is evident from Fig. 3 that the peak intensity variation consists of a succession of peaks as a function of aperture. These correspond to the fact that relative strengths of the maxima in the axial response change with aperture, so that the absolute maximum jumps from one maximum to an adjacent one.

The optimum phenomenon can also be observed when the two spherical aberration sources satisfy condition (7), i.e., the condition for aberration balance. In Figs. 2 and 3, $A = 100$ and $B = -26.66$. The optimum angle for the minimum half-width and the maximum peak intensity is now approximately 52°, close to the angle where the residual spherical aberration $\Phi_A + \Phi_B$ begins to increase appreciably (Fig. 1). For this special case, the optimum half-width can be more than halved, and the peak intensity can be increased by five times by use of the balancing condition.

This kind of improvement in axial response is not confined to this particular value when $A = 100$ but occurs over a wide range of A. In fact, for a given value of A, there is a corresponding optimum semiangular aperture for the half-width and the peak intensity. The relationship of optimum α to values of A is shown in Fig. 4 for the unbalanced ($B = 0$) and the balanced ($A = -3.75B$) cases. The optimum half-width and the peak intensity as functions of A are depicted in Figs. 5 and 6 for both cases, respectively.

3. Effect of the First Three Orders of Spherical Aberration

As shown in our previous results,[4] aberration compensation by altering the effective tube length is not complete, as we have 1 deg of freedom with which to cancel the aberration. For example, the primary and the fifth-order spherical aberrations can be balanced, but the higher-order spherical aberration terms remain. To understand the effects of these different terms on the axial response, we can expand[4] the aberration function Φ_A as a power series in s:

$$\Phi_A = A(1 + 2s^2 + 4s^4 + 8s^6 + \cdots + 2^n s^{2n} + \cdots), \quad (8)$$

where

$$s = \sin(\theta/2), \quad (9)$$

and the terms in powers of s^2, s^4, and s^6 are called the defocus, the primary, and the fifth-order aberrations, respectively. The remaining terms we call the higher-order aberrations.

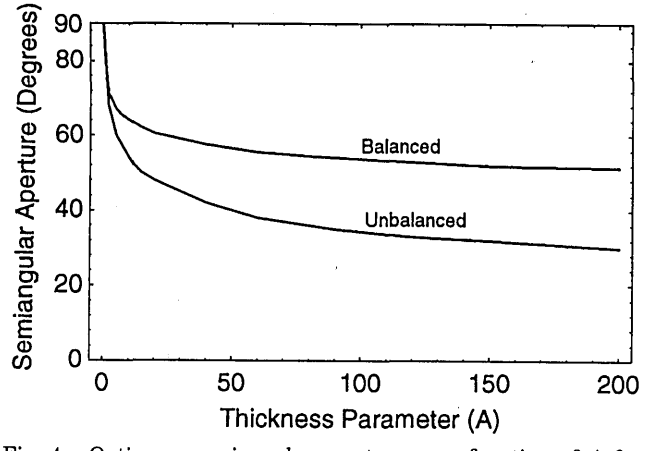

Fig. 4. Optimum semiangular aperture as a function of A for unbalanced and balanced cases.

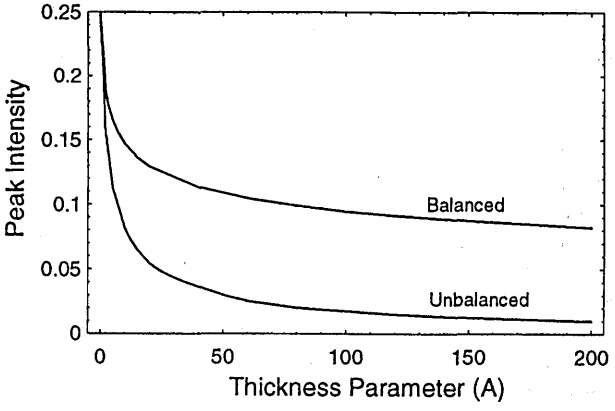

Fig. 6. Optimum peak intensity as a function of A for unbalanced and balanced cases.

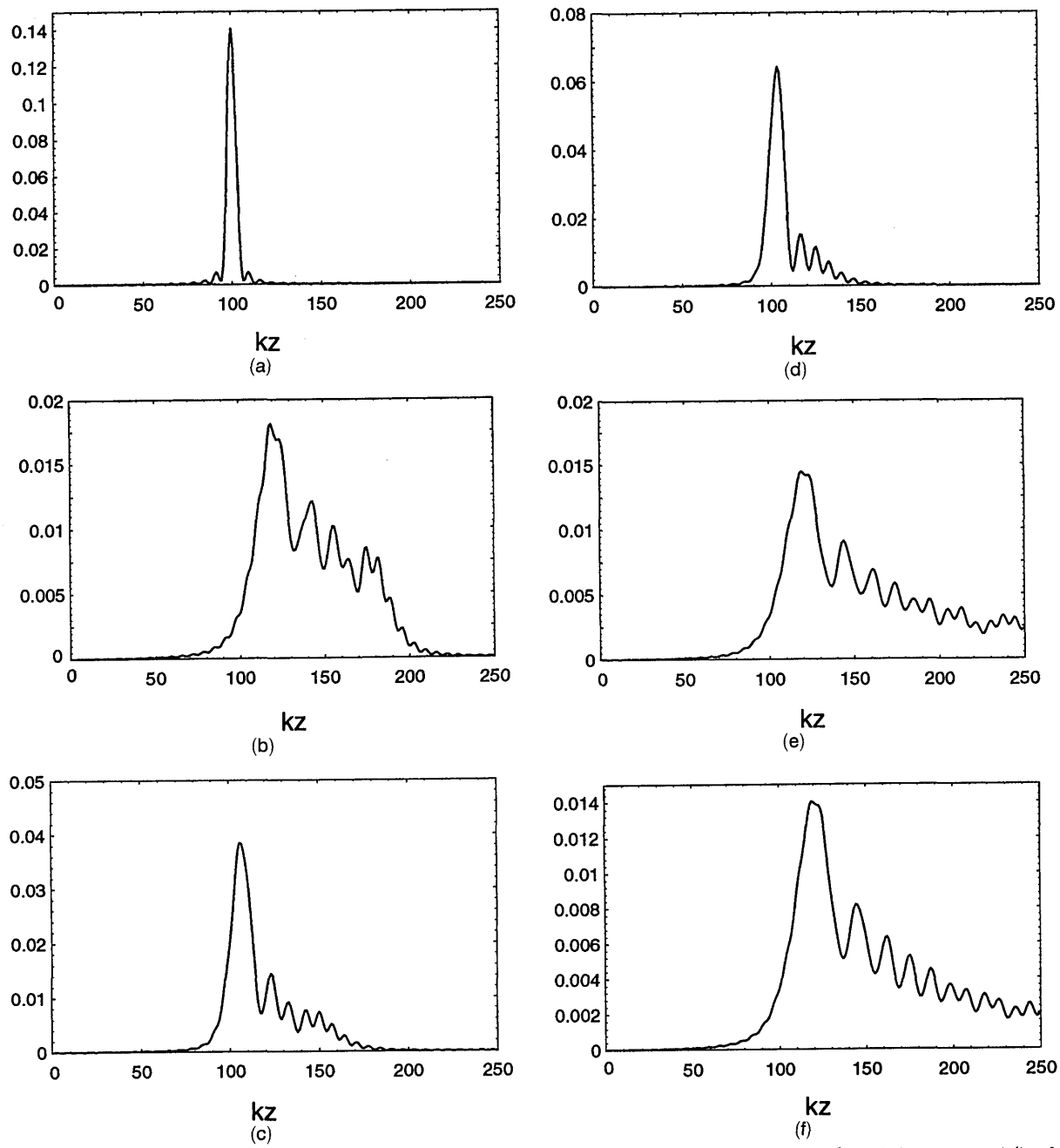

Fig. 7. Axial responses when $A = 100$: (a) including the defocus (s^2) term; (b) including the defocus (s^2) and the primary (s^4) spherical aberration terms; (c) including the defocus (s^2) and the fifth-order (s^6) spherical aberration terms; (d) including the defocus (s^2) and the seventh-order (s^8) spherical aberration terms; (e) including the defocus (s^2), the primary (s^4), and the fifth-order (s^6) spherical aberration terms; (f) including the defocus (s^2), the primary (s^4), the fifth-order (s^6), and the seventh-order (s^8) spherical aberration terms.

For $A = 100$ and $\alpha = 60°$, the axial responses are shown in Fig. 7 for various cases. The axial responses are represented in arbitrary units. The magnitude of the intensity denotes the relative strength of the response. The constant term in Eq. (8) represents a constant phase that does not contribute to the axial response. The defocus term ($2As^2$) produces only a shift of the origin in the axial response [see Fig. 7(a)], compared with the result for the aberration-free case.[4] The primary spherical aberration strongly degrades the axial response [see Fig. 7(b)]: strong sidelobes around the central peak are observed, the intensity of the central peak is decreased, and the half-width of the central peak is increased. It should be noted that the axial response with just primary spherical aberration is not symmetrical because of the apodization for an aplanatic system of high aperture [Eq. (1)]. The influence of the fifth- and the seventh-order terms is less strong than that of the primary spherical aberration [see Figs. 7(c) and 7(d)]. In fact, the half-width is increased by only 85% when the seventh order is

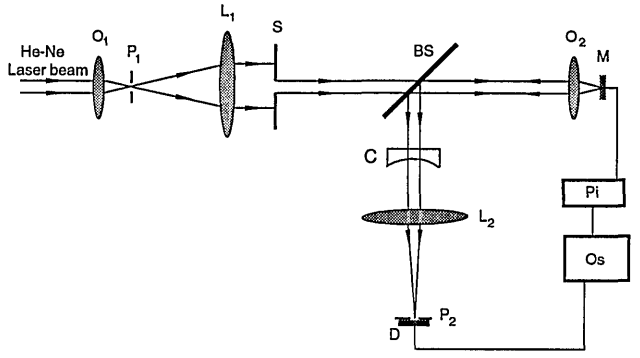

Fig. 8. Experimental setup: O_1, O_2, objectives; L_1, L_2, lenses; C, correction lens; P_1, P_2, pinholes; D, detector; BS, beam splitter; S, diaphragm; M, mirror acting as an object; Os, oscilloscope; Pi, piezodriver.

included. The axial response in the presence of the primary and the fifth-order spherical aberrations is further degraded [see Fig. 7(e)]: the peak intensity is further dropped, and the sidelobes extend over a wider range. When the seventh-order spherical aberration is also included, the axial response is almost the same as that when Eq. (2) is used.[4] The conclusion is that the higher-order spherical aberrations produce only a weak influence on the axial response. This is the reason that a good axial response can be obtained by alteration of the effective tube length to compensate for primary and fifth-order spherical aberrations.

It is seen that the theoretical axial response for primary spherical aberration only is much more irregular than is seen in practice. The addition of the fifth-order spherical aberration term [Fig. 7(c)] makes the response much more similar to the experi-

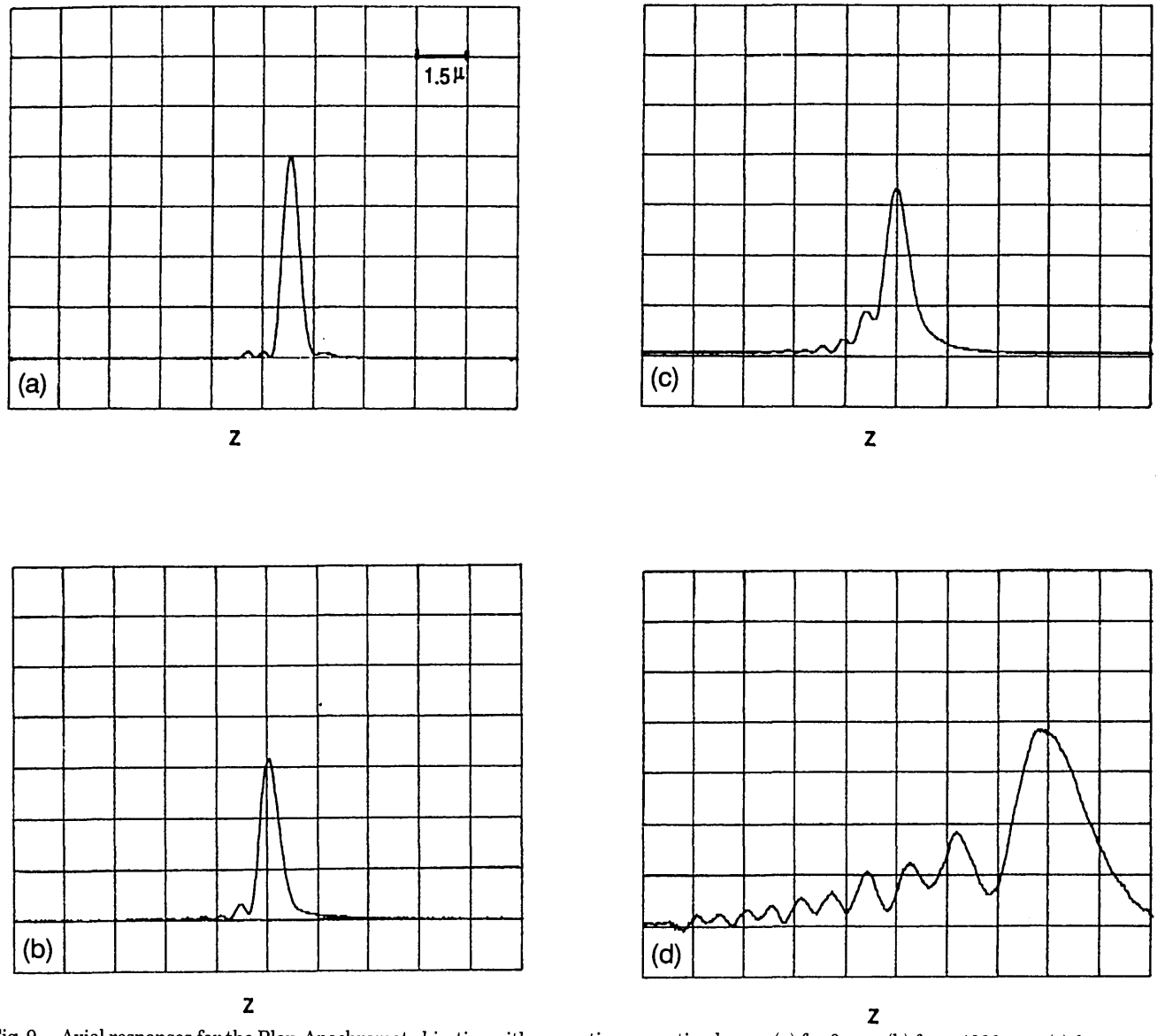

Fig. 9. Axial responses for the Plan-Apochromat objective with a negative correction lens: (a) $f = 0$ mm, (b) $f = -4000$ mm, (c) $f = -2000$ mm, (d) $f = -1000$ mm.

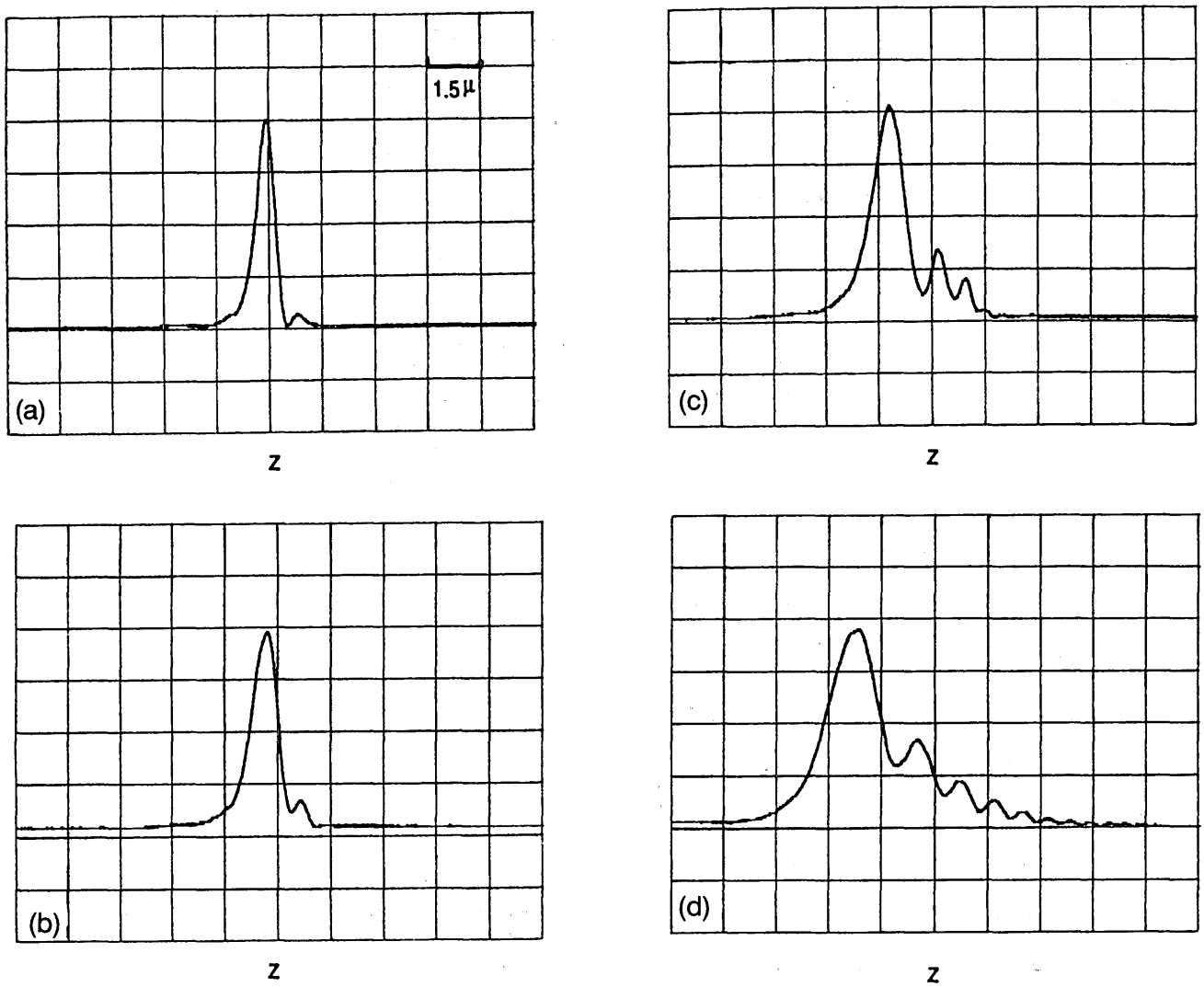

Fig. 10. Axial responses for the Plan-Apochromat objective with a positive correction lens: (a) $f = 4000$ mm, (b) $f = 2000$ mm, (c) $f = 1000$ mm, (d) $f = 500$ mm.

mental ones. This suggests that the fifth-order term is important in describing the behavior.

The results can be explained by application of the principle of stationary phase,[9] according to which, for strong aberrations, the integral in Eq. (1) can be approximated by the sum of three components, one from each of the limits of integration and one from the value of θ from which the phase exhibits a stationary value, if any. As z changes, the value of θ for the stationary point changes from zero to α. The component from the stationary point is the dominant term, the strength of which decreases as a result of the $\cos\theta$ weighting in Eq. (1) caused by the sine condition being satisfied, from the paraxial to the marginal focus. Thus the peak of the axial response occurs close to the paraxial focus. The relative strengths of the components from the integration limits are also affected by the weighting so that the contribution from the paraxial limit is larger. If the rate of change of phase at the pupil edge is large, then the contribution from the marginal limit is negligible, so that the resultant response is given by interference between the strong stationary component and a weaker paraxial component. This is approximately the case in Figs. 7(c)–7(f). If the rate of change of phase is smaller at the edge of the pupil, there is interference between all three components, and the response is more irregular in nature [as in Fig. 7(b)]. Thus addition of the higher orders of spherical aberration results in the behavior observed in practice.

It should be noted that the presence of the pupil weighting caused by the lens satisfying the sine condition results in substantially different behavior from that predicted by a normal small aperture approximation. The latter predicts a disk of least confusion in the point-spread function midway between the paraxial and the marginal foci, whereas for the sine condition case for strong aberration, the disk of least confusion is close to the paraxial focus.

These arguments also help explain the behavior described in Section 2. As the contribution to the

integral from the marginal limit is negligible, then above some value for the numerical aperture (which depends on the strength of the aberration) the aperture does not affect the axial response significantly.

Experimental investigations of both the focusing through a dielectric slab and the alteration of tube length give axial responses of a smoothly oscillating form rather than the more irregular behavior seen with primary spherical aberration only. If the objective lens accurately obeys the sine condition, then only primary spherical aberration is introduced on a change of tube length. This suggests that commercial microscope objectives do not accurately obey the sine condition. However, as we have no design data for the microscope objective used it is difficult to compare our results with theoretical predictions. In Section 2 we assumed for compensation of the axial response that the objectives obeyed the Helmholtz tangent condition, and this has been found to give reasonably good agreement with observed results.

4. Experimental Results

Although some experimental results concerning the axial response in the presence of spherical aberration have been reported elsewhere,[5,6] we demonstrate, in particular, the effect of the tube length on the axial response and the improvement in the axial response by the reduction of the lens aperture size.

The experimental setup for measuring the confocal axial response is illustrated in Fig. 8. Light from a He–Ne laser ($\lambda = 0.6328$ μm) is focused by objective O_1 onto pinhole P_1 with a radius of 10 μm. It is then collimated by lens L_1 with a focal length of 200 mm. Diaphragm S was effectively used to adjust the diameter of the entrance pupil of the objective. After passing through diaphragm S, the beam is then focused by microscope objective O_2 onto a mirror that is controlled by a piezodriver and thus scanned along the axial direction. The signal reflected from the scanned mirror is finally focused onto another pinhole, P_2, with a radius of 5 μm in front of photodiode detector D by another collimating lens, L_2, with a focal length of 200 mm. The detected signals, i.e., the axial responses of the mirror, are displayed on the screen of an oscilloscope.

Two microscope objectives (O_2) were used in the experiments: one was a Plan-Apochromat oil-immersion objective of numerical aperture 1.4, and the other was a Plan-NeoFluar dry objective of numerical aperture 0.75. Both are designed to be operated at an infinite tube length.

It is seen that our experimental setup is designed to use collimated beams. When the Plan-Apochromat objective is used, no aberration is caused by the optical system because it is operated at a correct tube length. As a result, the axial response in this case is almost symmetric and has small sidelobes [see Fig. 9(a)]. The value of the full width at half-maximum (FWHM) of the axial response is ~0.57 μm, which is larger than the theoretical value of 0.39 μm. This is a tendency we have observed previously from highly corrected Plan-Apochromat objectives.[10]

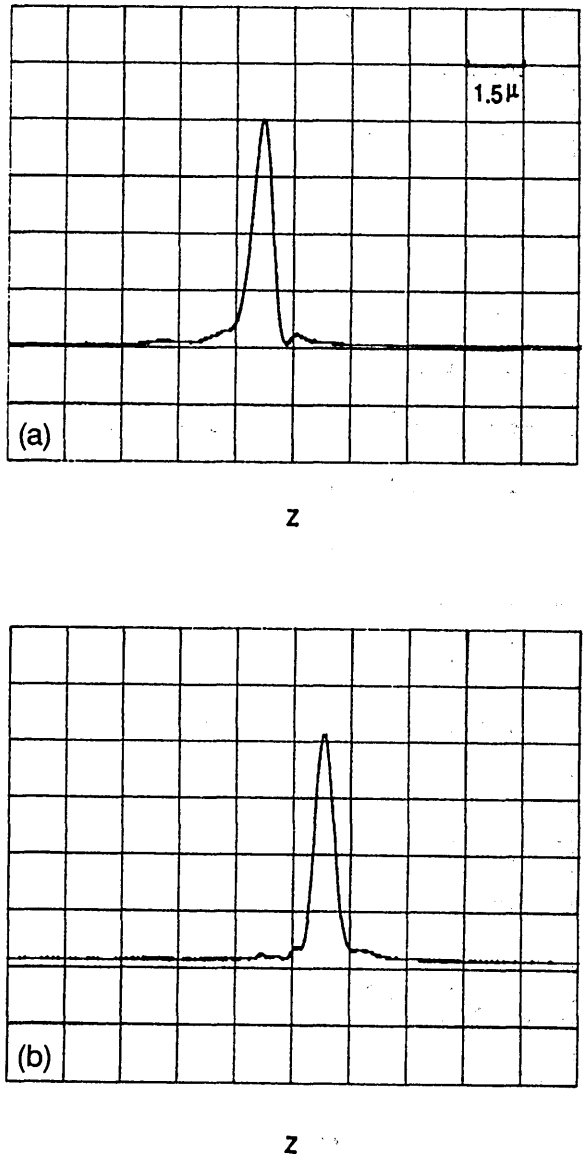

Fig. 11. Axial responses for the Plan-Apochromat objective with a cover glass: (a) without any correction lens, (b) with a negative correction lens ($f = -4000$).

To observe the effect of the effective tube length on the axial response, we inserted a correction lens (C) in front of objective O_2. One can alter the effective tube length at which the objective is operated by changing the focal length and the position of the correction lens. If the correction lens is weak, its position is not critical. The axial responses obtained when a correction lens of a negative focal length f is used are shown in Figs. 9(b)–9(d), while Fig. 10 represents those obtained when a correction lens of a positive focal length is used. The axial responses in the former case have sidelobes on the left-hand side of the main peak and those in the latter case have sidelobes on the right-hand side. This phenomenon can be understood from our previous investigations.[4] It has been shown[4] that the spherical aberration resulting from an alteration of the tube length is characterized by a

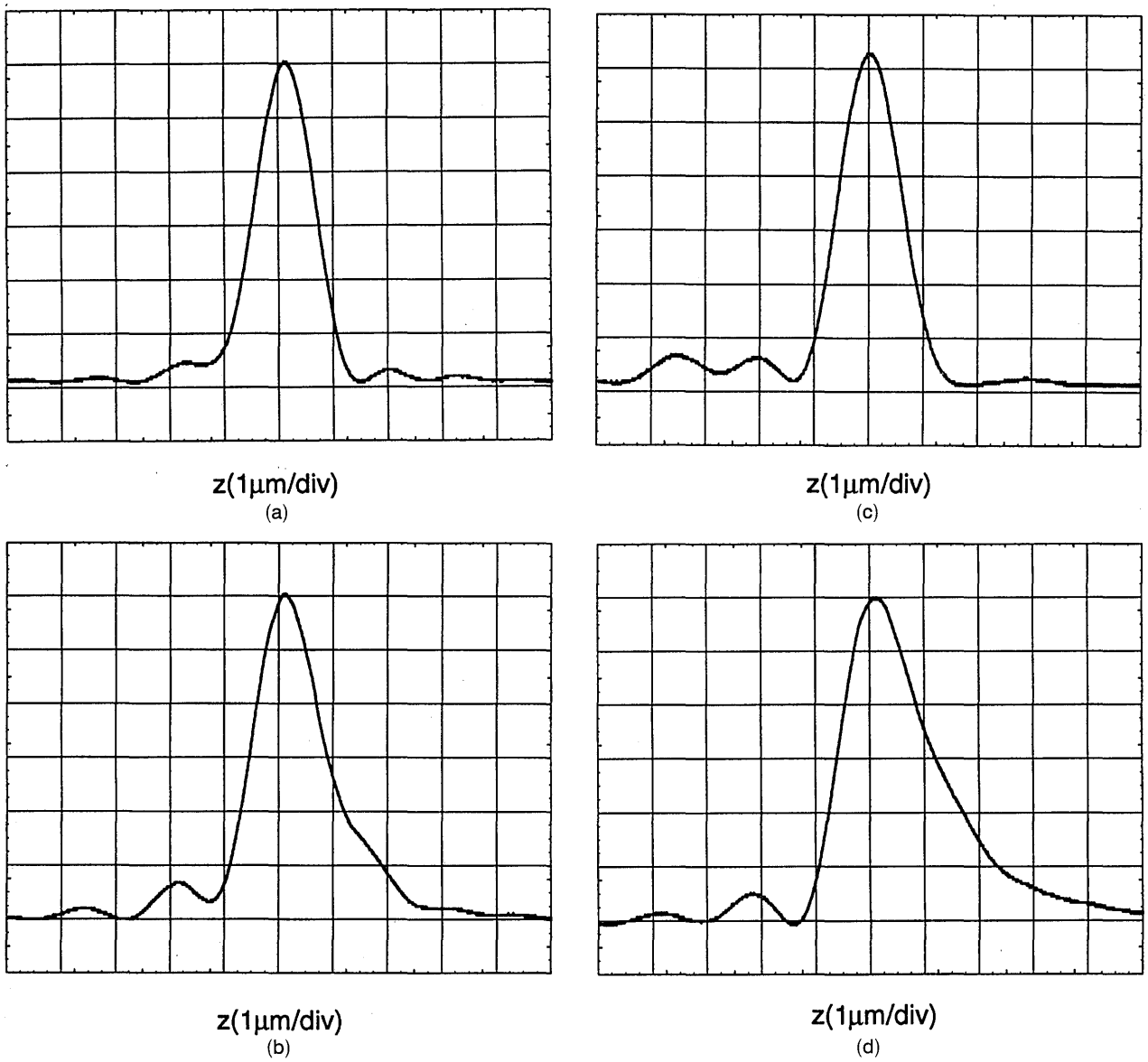

Fig. 12. Measured axial responses for different diameters (D) of the entrance pupil of the objective: (a) D = 6.5 mm with a number 1½ cover glass of thickness 0.17 mm, (b) D = 6.5 mm with a number 1 cover glass of thickness 0.12 mm, (c) D = 5 mm with a number 1 cover glass of thickness 0.12 mm, (d) D = 4.5 mm with a number 1 cover glass of thickness 0.12 mm.

parameter B [see Eq. (5)]. $B = 0$ represents the aberration-free case. When $B > 0$, the sidelobes appear on the right-hand side of the central peak, but the sidelobes appear on the left-hand side if $B < 0$. By using the formulas in Ref. 4, it can be estimated that the axial responses in Fig. 9 correspond, approximately, to $B = 0$ [Fig. 9(a)], -8.5 [Fig. 9(b)], -17 [Fig. 9(c)], and -34 [Fig. 9(d)], while those in Fig. 10 correspond to $B = 8.5$ [Fig. 10a], 17 [Fig. 10(b)], 34 [Fig. 10(c)], and 68 [Fig. 10(d)]. It is evident that when the aberration becomes strong, i.e., when the value of B is increased, the axial response is degraded: the central peak becomes broader, the sidelobes are stronger, and the minima are less pronounced. These properties are, on the whole, in agreement with the theoretical predictions[4] and imply that the commercial objective we used does not obey the sine condition, as discussed in Section 2.

Next, let us turn to aberration compensation. We introduced weak spherical aberration by putting a cover glass (number 1½) 0.15 mm thick on the top of the mirror. A few weak sidelobes appear on the right-hand side [see Fig. 11(a)] because of the presence of the spherical aberration resulting from the slight mismatch of the refractive indices between the cover glass and the immersion oil. As a result, the FWHM of the axial response is increased to 0.67 μm. According to our previous result,[6] the refractive-index mismatch Δn is approximately 0.02, so that the value of A in the present case is ~ 45. To compensate for the aberration caused by the insertion of the cover glass, we should alter the optimum tube length

at which the objective is operated to a new value. It was found that inserting a negative lens with a focal length of −4000 mm resulted in an optimum axial response with a value for the FWHM of 0.59 μm [see Fig. 11(b)], close to that in Fig. 9(a). Thus the experimental value of the ratio of A to B for aberration compensation is ~5.2, which is larger than the theoretical prediction.

The Plan-NeoFluar dry objective was used to study the effect of the lens aperture size. We adjusted the diameter of the diaphragm to 6.5 mm in order that the light beam could just fully illuminate the entrance pupil of the objective. The measured axial responses for different diameters of the diaphragm are shown in Fig. 12. Because the objective is designed to be used with a cover glass 0.17 mm thick, the axial response with a number 1½ cover glass (the thickness of the glass is ~0.17 mm in the experiment) is less aberrated with a half-width of 1.09 μm [Fig. 12(a)]. The signal becomes asymmetric, and its half-width is ~1.26 μm when a number 1 cover glass 0.12 mm thick is employed [Fig. 12(b)] as a result of the spherical aberration. By slightly reducing the diameter to 5 mm, we obtained a symmetric axial response, the half-width of which is approximately 1.15 μm [Fig. 12(c)]. The further reduction of the lens aperture size results in the broad and asymmetric signal again [Fig. 12(d)]. These results qualitatively demonstrate our theoretical prediction that the aberrated axial response can be improved by the slight reduction of the lens aperture size. The further quantitative comparison of the experimental result with the theoretical relations in Section 2 is difficult, as the strength of the aberration is unknown in the experiment.

5. Summary

The axial response in the presence of spherical aberration has been studied by inspection of the effects of the aperture size of the lens and the first three-order terms of the aberration. It is shown the axial response can be optimized by alteration of the aperture to an optimum value. This effect has been experimentally demonstrated. We also experimentally demonstrated the effect of the tube length on the axial response.

We thank the Australian Research Council and Science Foundation for Physics within the University of Sydney for support. M. Gu also acknowledges the support of an Australian Research Council Fellowship.

References

1. C. J. R. Sheppard, "Scanning optical microscopy," in *Advances in Optical and Electron Microscopy,* R. Barer and V. E. Cosslett, eds. (Academic, London, 1987), Vol. 10, pp. 1–98.
2. T. Wilson, *Confocal Microscopy* (Academic, London, 1990).
3. H. J. Matthews, D. K. Hamilton, and C. J. R. Sheppard, "Aberration measurement by confocal interferometry," J. Mod. Opt. **36,** 233–250 (1989).
4. C. J. R. Sheppard and M. Gu, "Aberration compensation in confocal microscopy," Appl. Opt. **30,** 3563–3568 (1991).
5. C. J. R. Sheppard and M. Gu, "Axial imaging through an aberrating layer of water in confocal microscopy," Opt. Commun. **88,** 180–190 (1992).
6. C. J. R. Sheppard and C. J. Cogswell, "Effects of aberrating layers and tube length on confocal imaging properties," Optik **87,** 34–38 (1991).
7. K. Carlsson, "The influence of specimen refractive index, non-uniform scanning speed, and detector signal integration on the imaging quality in confocal microscopy," Trans. R. Microsc. Soc. **1,** 219–222 (1990).
8. C. J. R. Sheppard and T. Wilson, "Effects of high angle of convergence on $V(z)$ in the scanning acoustic microscopy," Appl. Phys. Lett. **38,** 858–859 (1981).
9. M. Born and E. Wolf, *Principles of Optics* (Pergamon, Oxford, 1980), p. 752.
10. C. J. Cogswell, C. J. R. Sheppard, C. C. Moss, and C. V. Howard, "A method for evaluating microscope objectives to optimise performance of confocal systems," J. Microsc. **158,** 177–186 (1990).